III-1

Accelerators and Instruments

Light sources

Measurement of Temporal Response of Transmission-Type Spin-Polarized Photocathodes

T. Inagaki[1], N. Yamamoto[1], T. Konomi[2], Y. Okano[3], M. Adachi[4], X. G. Jin[1], M. Hosaka[1], Y. Takashima[1] and M. Katoh[2,3,1]

[1]*Nagoya University, Nagoya 464-8601, Japan*
[2]*UVSOR Facility, Institute for Molecular Science, Okazaki 444-8585, Japan*
[3]*Laser Research Center for Molecular Science, Okazaki 444-8585, Japan*
[4]*High Energy Accelerator Research Organization (KEK), Tsukuba 305-0801, Japan*

We have developed transmission-type spin polarized photocathodes with negative electron affinity (NEA). The spin-polarized electron beam is essential for "International Linear Collider" and so on. It is also expected to be applied for "Spin-resolved Inverse Photoemission Spectroscopy" [1].

In order to measure the temporal response of photocathodes, we developed the electron pulse length measurement system with 20 kV DC gun (Fig. 1). In this system by using an rf deflecting cavity, the electron beam is kicked transversely according to the rf phase position and the longitudinal pulse structure is projected to the transverse plane. We have employed the resonance mode of TM120. The resonance frequency is 2614 MHz for the rf cavity and the resonance frequency corresponds to the multiple of RF acceleration frequency of UVSOR storage ring, so the laser can be synchronized with UVSOR accelerator is used for the pump laser [2]. Temporal response of the photocathodes is evaluated by comparing the electron pulse structure and the pump laser pulse length. The pump laser pulses are provided by a mode-locked Ti:sapphire oscillator. In the present system by using a pulse stretcher, the pulse length of the pump laser can be selected in the range between 6.1 and 45 ps.

After the installation of the rf cavity to electron gun system, we carried out the measurement test with the GaAs/GaAsP superlattice photocathode with thickness of 96 nm. To evaluate its temporal response, the longitudinal pulse structure of electron beam projected by an rf deflecting cavity is fitted with a temporal response function which has two decay time constants, fast and slow temporal response times (Fig. 2). The measurement is carried out with pump laser length of less than 10 ps. As the results, two decay time constants are 3.1 ± 0.9 and 14 ± 1 ps, respectively. We considered that this result is consistent in a prior research with almost the same active layer thickness on front irradiation type [3].

Finally, in near future we are planning to reduce electron beam size before it is projected to the transverse plane in order to realize more precisely temporal response measurement and we will make systematic measurement for the various transmission-type photocathodes.

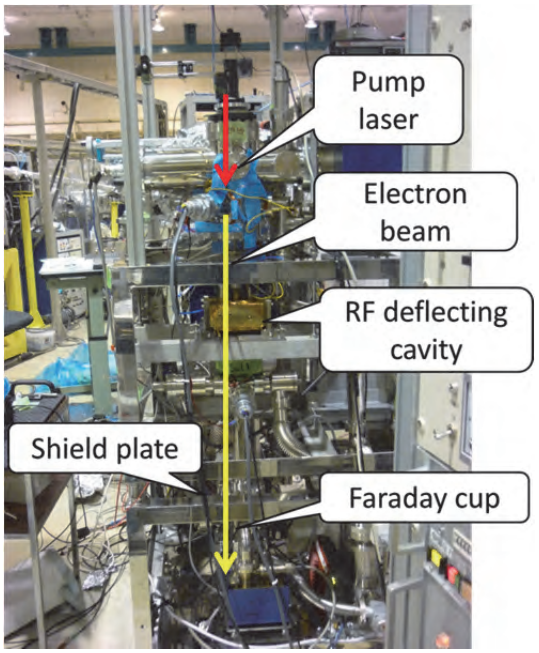

Fig. 1. 20 kV DC electron gun.

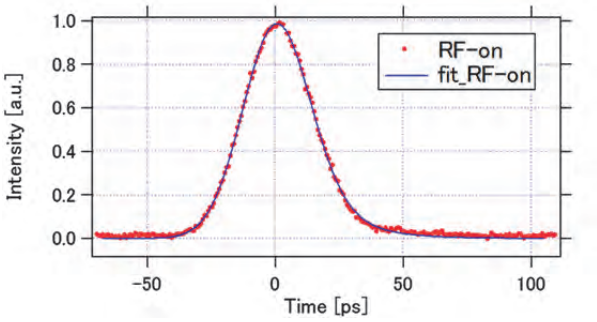

Fig. 2. Experimental data and fitted curves for a longitudinal pulse structure of electron beam.

[1] N. Yamamoto, doctoral thesis, Nagoya University (2007).
[2] T. Niwa, master's thesis, Nagoya University (2013).
[3] X. G. Jin *et al.*, "Picosecond electron bunches from GaAs/GaAsP strained superlattice photocathode" *Ultramicroscopy* **130** (2013) 44.

Light Sources

Narrow Band Coherent Edge Radiation from UVSOR-III Storage Ring

M. Hosaka[1], D. Oodake[2], N. Yamamoto[1,2], T. Konomi[3,4], J. Yamazaki[3], K. Hayashi[3], Y. Takashima[1,2] and M. Katoh[3,4]

[1]*Synchrotron Radiation Research Center, Nagoya University, Nagoya 464-8603, Japan*
[2]*Graduate School of Engineering, Nagoya University, Nagoya 464-8603, Japan*
[3]*UVSOR Facility, Institute for Molecular Science, Okazaki 444-8585, Japan*
[4]*School of Physical Sciences, The Graduate University for Advanced Studies (SOKENDAI), Okazaki 444-8585, Japan*

We have already succeeded in producing narrow band coherent THz radiation by manipulating the interaction between a relativistic electron bunch and an amplitude modulated laser [1]. In the former experiment, the radiation from a bending magnet where electrons moving along a circular trajectory, is extracted. As next step we planned to extract the radiation from edges of bending magnets, where electrons experience rapid change of magnetic field. The radiation is called edge radiation and has distinctive features as compared to normal synchrotron radiation: highly collimation even in long wavelength region, annular radiation pattern and radial polarization. Applying our technique of amplitude modulation laser, intense narrow band edge radiation is expected to be generated. Moreover, radially polarized light can be converted to Z-polarized one by using a high NA lens. Novel new applications of the radiation, such as surface science and solid state physics are expected.

The experiment to observe narrow band edge radiation was carried out with an electron beam of 600 MeV. Amplitude modulated Ti:Sa of 3 mJ was injected to BL1U undulator where the interaction between the laser and the electron bunch occurs. We have installed a simple beamline consisting of a mirro and a window port at 0 degree of BL2 to extract edge radiation from the edges of the bend 1 and bend 2. The edge radiation from the beamline was detected using an InSb hot-electron bolometer. In the initial experiment, we confirmed that the radiation intensity is proportional to the square of stored beam current, as is peculiar to coherent radiation (the figure is not seen in this report). Then we measured radiation intensity as a function of the THz frequency adjusted by the laser modulation frequency. Figure 1 shows the experimental result compared with efficiency calculations taking account of optical parameters of UVSOR-III magnetic lattice. As seen in the figure they agree well except for very low frequency region (~ 5 cm^{-1}) where multi-turn effect [2] dominates, which we did not take into account in the calculation. We observed spatial intensity distribution of the radiation by moving the bolometer which is located at distance of about 7 m from the radiation source point.

In the experiment, we employed a polarizer to extract only horizontal polarized component. Figure 2 shows the spatial distribution obtained in the experiment with the wavelength adjusted to 20 cm^{-1}. We expected horizontally separated distribution (Fig. 2 (b)); however, the experimental result does not clearly reproduce the expected distribution. We think the spatial distribution is affected by diffraction due to a narrow beam duct. We are planning a similar experiment with shorter THz wavelength. We are also going to make a simulation taking account of the diffraction effect.

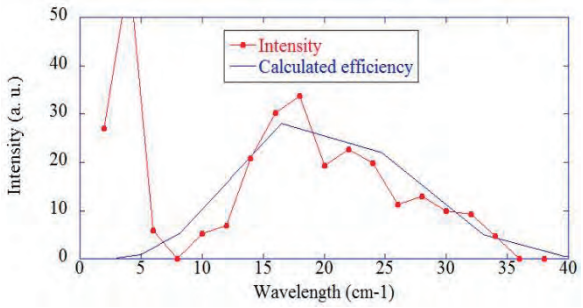

Fig. 1. Intensity of edge radiation as a function of wavelength.

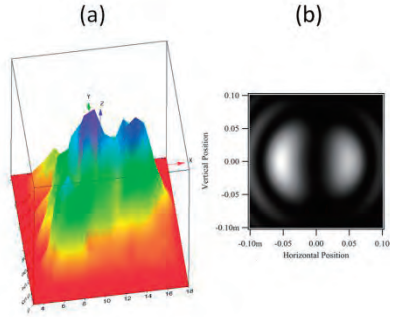

Fig. 2. Spatial distribution of horizontal polarized componet of edge radiation: (a) experiment (b) calculation.

[1] S. Bielawski *et al*., Nat. Phys. Rev. Lett. **4** (2008) 390.
[2] C. Evain *et al.,* Phys. Rev. ST Accel Beam **12** 9 (2010) 090703.

Light sources

Beam Injection with a Pulsed Multipole Magnet at UVSOR-III

N. Yamamoto[1], H. Zen[2], M. Hosaka[1], M. Adachi[4], K. Hayashi[3], J. Yamazaki[3], Y. Takashima[1] and M. Katoh[3,1]

[1]*Synchrotron Radiation Research Center, Nagoya University, Nagoya 464-8603, Japan*
[2]*Institute of Advanced Energy, Kyoto University, Uji 611-0011, Japan*
[3]*UVSOR Facility, Institute for Molecular Science, Okazaki, 444-8585, Japan*
[4]*High Energy Accelerator Research Organization, Tsukuba 305-0801, Japan*

The pulsed multipole injection scheme was developed at KEK-PF and KEK-AR [1,2]. In this scheme, the injection beam is captured into the accelerator acceptance as a result of pulsed multipole kicks, and the stored beam passes through the center of the multipole magnet, where the field strength is almost zero. The scheme thus avoids exciting coherent oscillation in the stored beam and delivers a high quality photon beam for synchrotron radiation users.

To introduce pulsed multipole injection into the UVSOR-III storage ring, we designed a rectangular-shaped pulsed multipole magnet (Fig.1) and tested it for electron beam injection[3]. The goal of the design was to compensate for residual magnetic fields by using thin ferrite bars applied to the pre-manufactured magnet.

The injection experiments demonstrated that multiturn injection, which uses the pulsed multipole magnet, is successful technique for UVSOR-III. This is the successful result of the pulsed multipole injection in case of as many as 7–9 kicks being applied to the same injected bunch on consecutive turns.

After optimizing the injection conditions, we obtained a maximum injection efficiency of 23% and an electron beam injection up to 300 mA. The injection efficiency obtained was less than expected from beam simulations, but the efficiency was sufficient to maintain the top-up operation at 300 mA. We suggest that the quality of the injection beam may have caused the lower injection efficiency because an injection efficiency lower than expected also occurred when using conventional dipole magnets. Thus, to obtain a higher injection efficiency, we shall focus our future investigations on the injector system.

Finally, this work demonstrates that the field-compensation technique based on using thin ferrite bars to cancel the residual magnet field is an economical and powerful way to improve performance. Coherent oscillations were drastically suppressed by applying this technique to pre-manufactured magnet (Fig. 2).

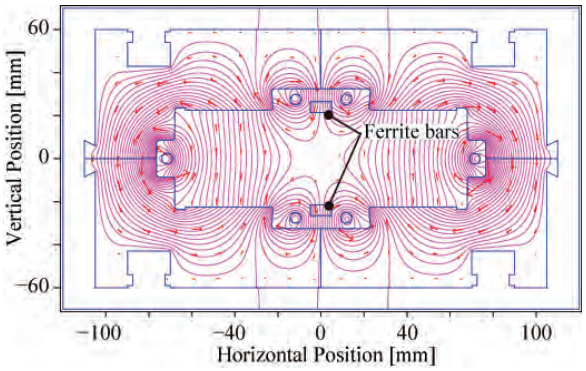

Fig. 1. Cross-section of the pulsed multipole magnet with calculated magnetic field.

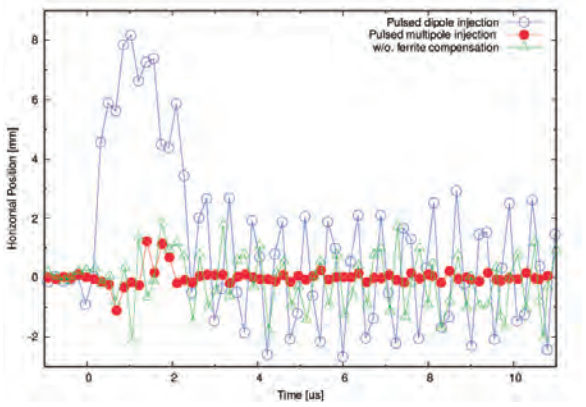

Fig. 2. Measured stored beam movements with pulsed dipole magnet (open circles) and pulsed multipole magnet with ferrite bars (close circles) and without ferrite bars (open triangles).

[1] K. Harada, Y. Kobayashi, T. Miyajima and S. Nagahashi, Phys. Rev. ST-AB **10** (12) (2007) 123501.
[2] H. Takaki, N. Nakamura, Y. Kobayashi, K. Harada, T. Miyajima, A. Ueda, S. Nagahashi, M. Shimada, T. Obina and T. Honda, Phys. Rev. ST-AB **13** (2010) 020705.
[3] N. Yamamoto, H. Zen, M. Hosaka, T. Konomi, M. Adachi, K. Hayashi, J. Yamazaki, Y. Takashima and M. Katoh, Nucl. Inst. and Meth. A **767** (2014) 26.

Others

Performance Evaluation of Mass Production Nuclear Emulsion for 2015 Balloon-Borne Experiment

N. Otsuka[1], H. Kawahara[1], H. Rokujo[1], K. Ozaki[2], S. Aoki[2], E. Shibayama[2], S. Takahashi[2], S. Tawa[2], F. Mizutani[2], K. Yamada[2], Y. Tateishi[2], T. Kosaka[2] and GRAINE collaboration

[1]*Graduate School of Science, Nagoya University, Nagoya 464-8602, Japan*

[2]*Department of Human Environment Science, Kobe University, Kobe 657-8501, Japan*

We are promoting GRAINE project. GRAINE project is a balloon-borne experiment to explore the gamma-ray astrophysics. We load a balloon with nuclear emulsion to observe cosmic gamma-rays. Nuclear emulsion is able to record the 3-dimensional trajectory of a charged particle within a 1-um accuracy. Nuclear emulsion is made of a plastic base and silver halide emulsion which is coated on a plastic base. After development the emulsion films, we can observe track made of silver grain by charged particles under a microscope. We observed electron-pair which created of cosmic gamma-rays in emulsion and reconstruct each gamma-ray to determine which way the gamma-ray come from. Figure 1 shows how track of charged particle look like in nuclear emulsion under microscope.

We produced nuclear emulsion at Nagoya University for next balloon-borne experiment. Next balloon-borne experiment will operate in May 2015, Australia. We were required to product about fifty square meters of nuclear emulsion for 2015 experiment. Mass production of silver halide emulsion for 2015 experiment is started at February 2014 and it finished in January 2015. Figure 2 shows time profile of the total amount of produced emulsions. We produce emulsion with R&D machine (1L tank) until November 2014. Thereafter, we introduced mass production machine (3L tank).

We need to evaluate performance of each silver halide emulsion. I will explain how to evaluate performance of silver halide emulsion. We expose electron beam to films made of silver halide emulsion to evaluate at UVSOR. Exposed film has trajectories of electron. We measured Grain Density (GD), counts of silver grains per 100um, by observed trajectories in emulsion under microscope. GD would be high when emulsion has high sensitivity to charged particle.

Figure 3 shows results of measurement of GD for all emulsions. The high density silver halide emulsion has an average GD of 50.6 and the middle density silver halide emulsion has an average GD of 45.8. Since next experiment demand more than 40 for GD, mass production of emulsion was stable. Moreover, the mass production machine is able to produce emulsion as the R&D machine.

Sufficient performed emulsions were coated on plastic bases at Nagoya University. These films are become detector for 2015 experiment.

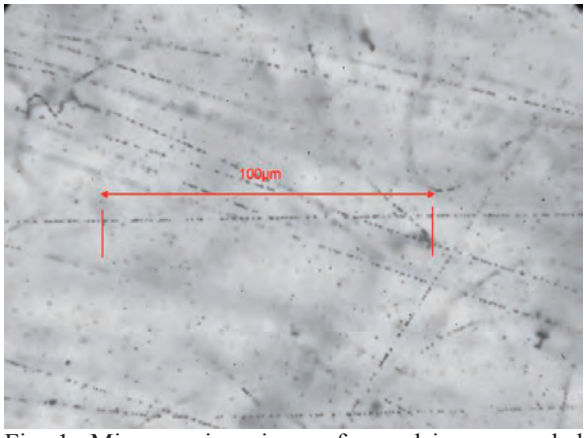

Fig. 1. Microscopic view of emulsion recorded charged track.

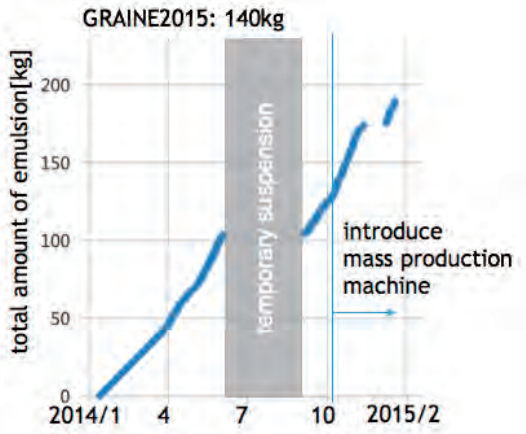

Fig. 2. Time profile of mass production for 2015 experiment.

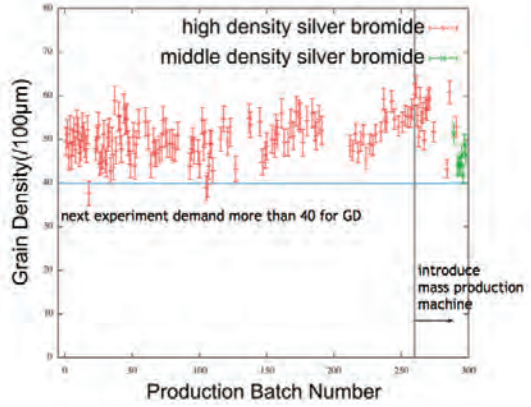

Fig. 3. Performance of produced silver bromide emulsions.

Others

Development of the Backward-Illuminated Photocathode for SRF GUN

T. Konomi[1], R. Inagaki[2], M. Hosaka[3], N. Yamamoto[3],Y. Takashima[2,3]and M. Katoh[1,3]
[1]*UVSOR Facility, Institute for Molecular Science, Okazaki 444-8585, Japan*
[2]*Graduate School of Engineering, Nagoya University, Nagoya 464-8603, Japan*
[3]*Nagoya University Synchrotron Radiation Research Center, Nagoya 464-8603, Japan*

Photocathode electron gun is a key component of the high brightness synchrotron radiation source such as free electron laser, energy recovery linac, etc. Superconducting RF gun has advantages on the high gradient and high duty operation because CW high power RF operation is capable. Figure 1 shows the superconducting RF gun cavity under development [1]. The cavity is made of pure niobium, and RF surface resistance is 1/1,000,000 compared with pure copper cavity. Therefore the gun can accelerate high current beam with high accelerating field.

Backward illumination with a transparent photocathode is desirable from the good laser operability point of view because it gives better laser pointing stability, laser shape operability with fiber bundle and a high numerical aperture lens. Figure 2 shows the shame of the gun. The excitation light (laser) is illuminated to the backside of the photocathode, and the electron beam emitted from front side of the photocathode and accelerated in RF field.

We studied the backward illumination for the transparent photocathode in a superconducting RF gun and we found that a combination of a transparent superconductor LiTi2O4 and the high brightness photocathode K_2CsSb is a candidate. Figure3 shows the structure of the photocathode. The transparent superconductor $LiTi_2O_4$ is epitaxially grown on transparent substrate $MgAl_2O_4$ [2]. RF is reflected at $LiTi_2O_4$ because RF Skin depth of the superconductor is several hundred nm. It's possible to protect the substrate with the insulation breakdown voltage.

Photocathode parameter was measured separately. The critical RF magnetic field was measured by SQUID (Fig.4). The operation RF magnetic field of SRF gun is 4.3 mT on the photocathode. The photocathode has double margin about RF field at 5K.

The quantum efficiency has the peak at green wavelength range (Fig.5).

We will develop SRF gun development such as laser development by using these cathode data.

Fig. 1. Superconducting RF gun cavity.

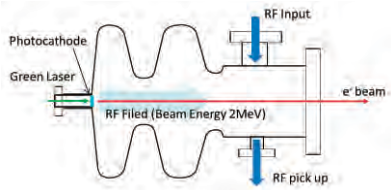

Fig. 2. Shame of developed electron gun.

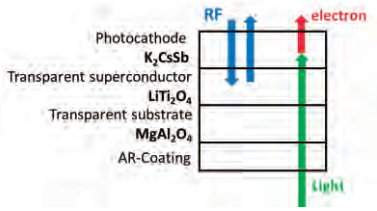

Fig. 3. The photocathode structure.

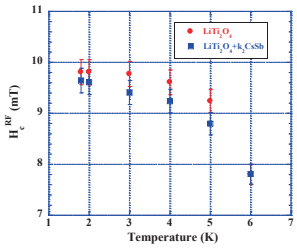

Fig. 4. Critical RF magnetic Field of LiTi2O4.

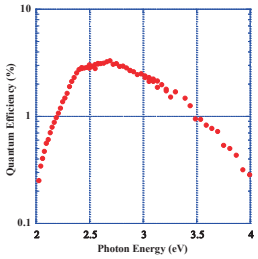

Fig. 5. Quantum efficiency of the photocathode.

[1] R. Matsuda *et al.*, PASJ11, MOOL13, 2014.
[2] A. Kumatani *et al.*, Appl. Phys. Lett. **101** (2012) 123103.

BL1U, Accelerators

Generation of Laser Compton Scattered Gamma-Ray Using a 1.95-μm Fiber Laser at UVSOR Facility

H. Zen[1], Y. Taira[2], T. Konomi[3,4], J. Yamazaki[3], T. Hayakawa[5], T. Shizuma[5], T. Kii[1], H. Toyokawa[2], M. Katoh[3,4] and H. Ohgaki[1]

[1]*Intitute of Advanced Energy, Kyoto University, Uji 611-0011, Japan*
[2]*National Institute of Advanced Industrial Science and Technology (AIST), Tsukuba 305-8568, Japan*
[3]*UVSOR Facility, Institute for Molecular Science, Okazaki 444-8585, Japan*
[4]*School of Physical Sciences, The Graduate University for Advanced Studies (SOKENDAI), Okazaki 444-8585, Japan*
[5]*Japan Atomic Energy Agency, Tokai-mura 319-1184, Japan*

High energy and quasi-monoenergetic gamma-rays can be generated by Compton backscattering between high energy electron beams and laser beams [1]. The gamma-rays are called as LCS (Laser Compton Scattering) gamma-ray and have unique and good features such as energy tunability, variable polarization and good directivity. Therefore, the LCS gamma-rays are very useful for various purposes. In order to generate narrowband and intense LCS gamma-ray, high current, low emittance and small energy spread electron beam must be provided.

In the UVSOR facility, high current (300 mA, top-up), low emittance (17.5 nm-rad) and small energy spread (5.26×10^{-4}) electron beam circulating in the UVSOR-III storage ring with electron energy of 750 MeV is available [2]. Those features of electron beam are very good for generating narrowband and intense LCS gamma-ray. Therefore, we proposed development of LCS gamma-ray source in the UVSOR facility.

In this fiscal year, we installed a 1.95-μm fiber laser in the downstream side of BL1U and performed LCS gamma-ray generation experiment. The experimental setup is shown in Fig. 1. Laser beam with 1.95-μm wavelength was injected from downstream side of BL1U and scattered by electron beam circulating in the storage ring. The characteristics of the fiber laser are listed in Table 1. The energy spectrum of generated LCS gamma-ray include detector efficiency is shown in Fig. 2. We have successfully generated LCS gamma-rays whose maximum energy of about 5.4 MeV. The gamma-ray yield with the beam current of 300 mA and laser power of 5 W is expected to be about 3×10^5 photons/s in 3% bandwidth.

Table 1. Characteristics of the 1.95-μm Fiber Laser

Parameter	Specification
Operation mode	CW
Operation wavelength	1950 nm
Max. output power	5 W
Spectral linewidth	< 1 nm
Beam quality, M^2	< 1.1
Output polarization	Linear

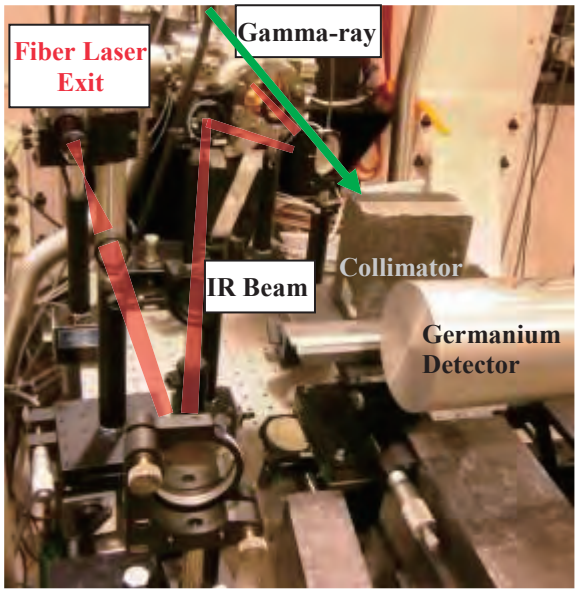

Fig. 1. Setup of LCS experiment at the downstream of BL1U.

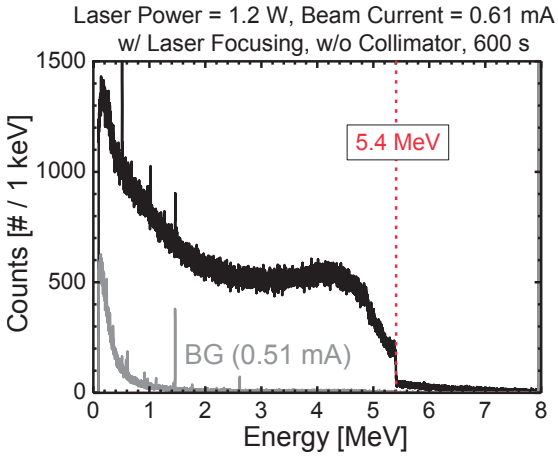

Fig. 2. Measured gamma-ray spectrum with and without laser injection.

[1] F. V. Hartemann *et al.*, Phys. Rev. ST Accel. Beams **8** (2005) 100702.
[2] M. Adachi *et al.*, J. Phys.: Conf. Ser. **425** (2013) 042013.

BL1U

Observation of Light's Orbital Angular Momentum from Helical Undulator Harmonics

S. Sasaki[1], A. Miyamoto[1], M. Hosaka[2], N. Yamamoto[2], T. Konomi[3] and M. Katoh[3]
[1]*Synchrotron Radiation Center, Hiroshima University, Higashi-Hiroshima 739-0046, Japan*
[2]*Nagoya University Synchrotron Radiation Research Center, Nagoya, 464-8603, Japan*
[3]*UVSOR Facility, Institute for Molecular Science, Okazaki, 444-8585, Japan*

The phenomenon of higher harmonic radiation from a helical undulator carrying orbital angular momentum (OAM)[1] attracts a great deal of attention because this novel property may be used as a new probe for synchrotron radiation science[2] that would be performed in a diffraction limited light source facility.

Although a diffraction limited x-ray source does not yet exist, the 750 MeV UVSOR-III is already a diffraction limited light source in the ultra violet (UV) wavelength region. In this ring, a tandem-aligned double-APPLE undulator system similar to that in BESSY-II [3] is installed for FEL and coherent light source experiments. Using this set-up, we observed spiral interference patterns between two different harmonic radiations with a scanning fiber multi-channel spectrometer and a CCD camera placed at the end of BL1U Beamline. By these measurements, various interference patterns such as single, double, and triple spirals were observed which concur with the theoretical prediction for every mode in the right or left circular polarization[4]. Figure 1 shows the layout of undulator system and beamline.

A schematic view of experimental set-up for the interference mesurements with a CCD cameara is shown in Fig. 2.

Figure 3 shows examples of interference patterns.

The rotation of an interference pattern by rotating a polarizer was also observed as shown in Fig.4.

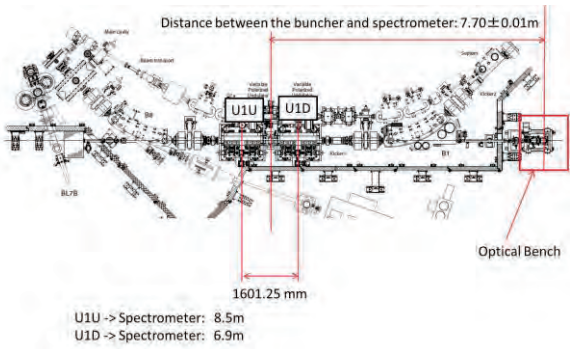

Fig. 1. Drawings of undulators and BL-1U beamline.

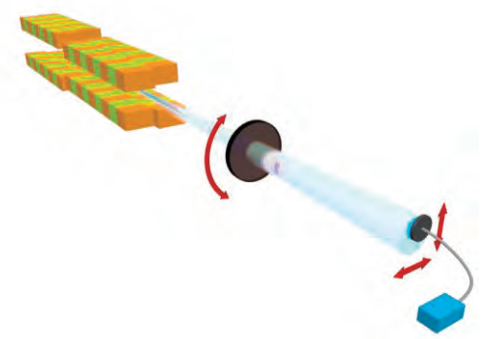

Fig. 2. Experimental set-up for interference measurements with a CCD camera.

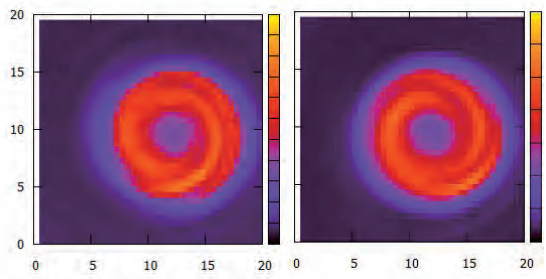

Fig. 3. Double spiral by interference between 1st & 3rd harmonic. E = 500 MeV, ε_0 = 8 nmrad, λ= 250 nm.

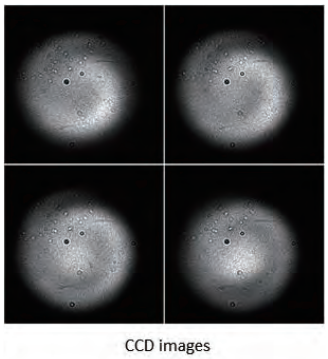

Fig. 4. Spiral rotation, 1st & 2nd harm.interference. Rot. Angle: TL: 0º, TR: 30º, BL: 60º, BR: 90º.

[1] S. Sasaki and I. McNulty, Phys. Rev. Lett. **100** (2008) 124801.
[2] M. VanVeenendaal and I. McNulty, Phys. Rev. Lett. **98** (2007) 157401.
[3] J. Bahrdt, *et al.,* Phys. Rev. Lett. **111** (2013) 034801.
[4] S. Sasaki, A. Miyamoto, M. Hosaka, N. Yamamoto, T. Konomi and M. Katoh, to be published.

BL2B

Reconstruction of the Beamline BL2B for Development of Photoelectron Spectroscopy for Organic Materials II

S. Kera[1,2], K. R. Koswattage[3], K. Yonezawa[2], Y. Nakayama[2], K. K. Okudaira[2] and H. Ishii[2,3]
[1]*Institute for Molecular Science, Okazaki 444-8585, Japan*
[2]*Graduate School of Advanced Integration Science, Chiba University, Chiba 263-8522, Japan*
[3]*Center for Frontier Science, Chiba University, Chiba 263-8522, Japan*

The beamline BL2B has been reconstructed for characterizing the wide range of molecular materials *via* angle-resolved photoelectron spectroscopy (ARPES) to achieve the fundamental understanding of charge transport properties, adsorption properties, interface energetics, chemical reactivity and so on, since September 2013.

The BL2B originally consists of M0, and M1 pre-focusing mirrors, entrance slit, monochromator, movable exist slit and M4 refocusing mirror. The monochromator consists of G1, G2, and G3 spherical gratings and M2 and M3 plane mirrors system [1, 2]. The monochromator was designed to cover the energy range of 23 – 205 eV and used for gas phase experiments till 2012.

In the initial process, the beamline was mainly reconstructed solving a malfunction of the M2 and M3 mirror system in the monochromator, introducing a UHV chamber (monitoring chamber) downstream of the M4 mirror chamber, building a new interlock system, placing a new end-station for the ARPES equipped with a hemispherical analyzer (SCIENTA R3000) [3]. Then, the beam line was carefully aligned starting from adjusting M0, M1, and subsequently adjusting the optics in the monochromator and M4 mirror. A typical spot size after the M4 refocusing mirror is roughly estimated to be about 1.5 mm × 0.8 mm (vertical × horizontal) for exist slit of 300 μm by a four directional slit (in between the M4 mirror & the monitoring chamber) edges scan.

The photon flux for an exit slit width of 300 μm are estimated to be $1\times 10^{10} - 3\times 10^{10}$, $4\times 10^{10} - 2\times 10^{11}$, and $1\times 10^{10} - 2\times 10^{10}$ photons/s for G1 (80 – 150 eV), G2 (50– 120 eV) and G3 (25 – 55 eV) gratings, respectively using a silicon photodiode (AXUV-100, IRD) and Au mesh in the monitoring chamber. The estimated photon flux is one order of magnitude smaller than the expecting value from the references [1, 2] and the decrement may be due to contamination of the optics, a slight misalignment of the light and so on.

The contribution of the second order light was estimated to be 10% at 28 eV and it can be reduced to 2.4% by inserting a metal filter (Al20nm/Mg300nm /Al20nm/Ni70nm, LUXEL) in the monitoring chamber. The accuracy of the photon energy at 28 eV was checked by measuring Fermi edge of gold considering the first and second order light, leading a difference of -0.04 eV.

The beamline resolution was determined by measuring Fermi edge of gold at low temperature ~13 K. Refereeing a preciously determined energy resolution of the analyzer (ΛR=2.3meV at pass energy (E_p) of 2eV and analyzer slit of 0.2mm) by Xe gas cell experiments, the photon energy resolution is estimated to be 14 ± 1 meV at 28 eV, and the value is consistent with the literature (E/ΛE = 2,000 @Slit 500μm) [1]. Consequently, one can obtain the ARPES data for a Au(111) surface as shown in Fig.1.

M0 mirror is cooled by water cooling system to improve the stability of the synchrotron light, however currently the cooling system having a problem where the mirror system cannot be cooled. Thus, the stability of the photon energy and flux has been carefully checked repeatedly measuring the binding energy and intensity of Au 4f at the photon energy of 110 eV. The result confirms that a stability to a certain extent of the light for a 24 hours continuous measurements which may not be a drawback for future experiments at BL2B.

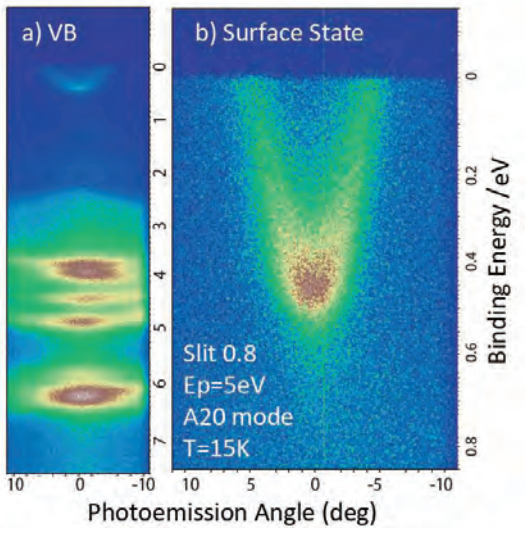

Fig. 1. ARPES of a clean Au(111) surface taken at 15 K and hν = 28 eV. (a) Valence band (VB) region is recorded for 5min and (b) surface state region is recorded for 40min to obtain an image.

[1] H. Yoshida and K. Mitsuke, J. Synch. Rad. **5** (1998) 774.
[2] M. Ono, H. Yoshida and K. Mitsuke Nucl. Instrum. Meth. Phys. Res. A **467-468** (2001) 577.
[3] S. Kera *et al.*, UVSOR Act. Repo2013 **41** (2014) 38.

BL6B, BL1U

Microbunching Instability in Relativistic Electron Bunches: Direct Observations of the Microstructures Using Ultrafast YBCO Detectors

E. Roussel[1], C. Evain[1], C. Szwaj[1], S. Bielawski[1], J. Raasch[2], P. Thoma[2], A. Scheuring[2], M. Hofherr[2], K. Ilin[2], S. Wünsch[2], M. Siegel[2], M. Hosaka[3], N. Yamamoto[3], Y. Takashima[3], H. Zen[4], T. Konomi[5], M. Adachi[5], S. Kimura[5] and M. Katoh[5]

[1]*Laboratoire PhLAM, Université Lille 1, 59655 Villeneuve d'Ascq, France*
[2]*Institute of Micro- and Nanoelectronic Systems, Karlsruhe Institute of Technology, 76187 Karlsruhe, Germany*
[3]*Synchrotron Radiation Research Center, Nagoya University, Nagoya 464-8603, Japan*
[4]*Institute of Advanced Energy, Kyoto University, Uji 611-0011, Japan*
[5]*UVSOR Facility, Institute for Molecular Science, Okazaki 444-8585, Japan*

During the synchrotron radiation process, each electron is exposed to the radiation emitted by the others. At high electron bunch charge, this collective effect is at the origin of an instability that leads to the spontaneous formation of spatial structures inside the electron bunch: the microbunching instability (or CSR instability). This very fundamental electromagnetic phenomenon is known as a limitation in various types of accelerators, and at the same time as a great opportunity for the generation of giant pulses of Terahertz radiation (Coherent Synchrotron Radiation or CSR). This phenomenon is also suspected to be at the origin of coherent emission in solar flares.

Although this is a well-known fact, direct experimental observations of the structures, or the field they emit (CSR), remained up to now an open problem. In the present work, we attempted to observe directly such a structure in a storage ring, and follow its evolution over many turns [1].

The experimental setup is displayed in Fig. 1. The UVSOR-III storage ring was operated in single bunch, above the microbunching instability threshold. The spontaneously formed structure (with ~9 mm wavelength) emitted a coherent radiation (at the same wavelength). This radiation was detected using an ultrafast detector developed by the Institute of Micro- and Nanoelectronic Systems (KIT, Germany). This detector has the capability to measure the total electric field evolution, with a time resolution that is better than fastest oscilloscope speeds (17 ps at the time).

The experimental recordings immediately revealed that we had access to the full shape of the CSR pulses (including envelope and carrier), and which are a direct "image" of the microstructures (Fig. 2). Then, the data quickly appeared as a powerful and severe reference for the tests of theoretical models. Comparison with numerical simulations quickly revealed model limitations, and how the models should be refined to reproduce the experimental data. These studies were also performed in presence of laser perturbations, using the slicing setup installed at BL1U (see Ref. [1] for details).

More generally, the possibility to "see" directly the microstructures shape and its evolution at each turn opens the way to tests of models, and control strategies that were not possible before.

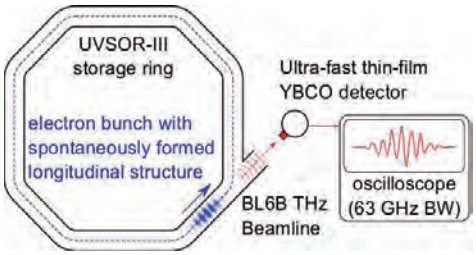

Fig. 1. Experimental setup.

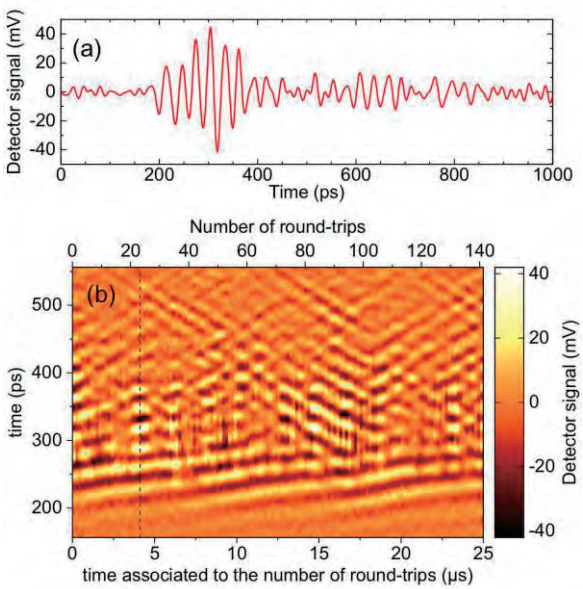

Fig. 2. (a) Typical pulse shape associated to a burst of CSR radiation that carries the information on the electron bunch microstructure. (b). Series of pulse shapes at successive round-trips in the ring.

[1] E. Roussel *et al.*, Phys. Rev. Lett. **113** (2014) 094801.
http://dx.doi.org/10.1103/PhysRevLett.113.094801.

BL7B

Evaluation of the VUV Coating Performed on the Flight Mirrors of the CLASP Sounding Rocket

N. Narukage[1], M. Kubo[1], R. Ishikawa[1], Y. Katsukawa[1], S. Ishikawa[1], T. Kobiki[1], G. Giono[1], R. Kano[1], T. Bando[1] and S. Tsuneta[2]

[1]*National Astronomical Observatory of Japan, Mitaka 181-8588, Japan*

[2]*Institute of Space and Astronautical Science, Japan Aerospace Exploration Agency, Sagamihara 252-5210, Japan*

Our team consisting of Japan, US, Spain, France, and Norway is developing a Chromospheric Lyman-Alpha SpectroPolarimeter (CLASP), which is proposed to fly with a NASA sounding rocket in 2015 [1, 2]. CLASP will explore the magnetic fields in the solar atmosphere (the upper chromosphere and transition region) via the Hanle effect in the Lyman-alpha (Lyα) line (121.6 nm) for the first time. This experiment requires precise spectropolarimetric observations with a polarimetric sensitivity of 3σ ~ 0.1% and a wavelength resolution of 0.01 nm.

In order to achieve the polarimetric sensitivity of 3σ ~ 0.1%, CLASP requires the high throughput for suppressing the photon noise. For this purpose, CLASP is consists of minimum number of reflective mirrors [3]. And, we have developed three types of high-efficiency VUV reflective coatings, namely, a reflective narrow band filter coating [4], a high reflectivity polarizing coating [5], and a high reflectivity mirror coating.

In 2014, we fabricated the flight mirrors and performed the high-efficiency VUV reflective coatings on such flight mirrors. In order to evaluate the performance of the flight coatings, witness samples (whose diameters are 1 inch or 30 mm) were coated simultaneously with the flight mirrors. Using these witness samples, we evaluated the performance of the flight coatings at UVSOR BL7B with our measurement system shown in Fig. 1 (see the details in Narukage *et al.* [5]).

The reflective narrow band filter coating was applied to the 290 mm diameter primary mirror (see Fig. 2). The measured reflectivity in Lyα is about 56%. Meanwhile, the reflectivity in visible light and infrared is less than 5 % in average. Hence, this coating can efficiently remove the unwanted visible light and heat, which are the dominant components in the solar spectrum. Additionally, this coating is enough uniform across the entire 290 mm diameter to suppress the polarization caused by the non-uniformity of the coating to less than 10^{-3} % [6].

The high reflectivity polarizing coating on the flight polarization analyzer has a performance of R_s ~ 55 % and R_p ~ 0.3 % at their Brewster's angle of 68 degree in Lyα, where R_s and R_p are reflectivity for s- and p-polarized beam, respectively. This coating has ~ 2.5 times higher efficiency than MgF_2, and high polarization power (≡ $(R_s–R_p) / (R_s+R_p)$) of 98.9 %.

Other mirrors, namely, secondary mirror and two camera mirrors, were coated with the high reflectivity mirror coating. The measured reflectivity is more than 80 % in Lyα.

On the bases of these measurements with BL7B, we confirmed that all of the coatings on the CLASP flight mirrors satisfy the specifications determined for the polarimetric sensitivity of 3σ ~ 0.1%.

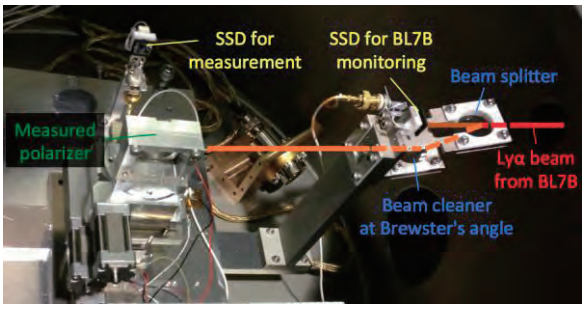

Fig. 1. Photo of our measurement system.

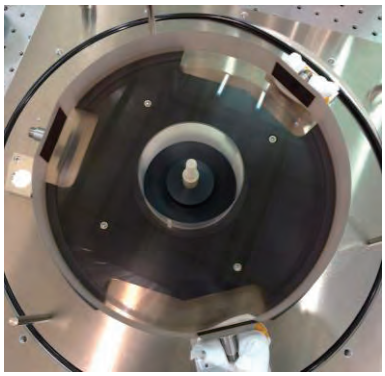

Fig. 2. Photo of the CLASP primary mirror.

[1] R. Kano *et al*., SPIE **8443** (2012) 84434F.
[2] K. Kobayashi *et al*., Proc. Fifth Hinode Science Meeting, Astronomical Society of the Pacific Conference Series **456** (2012) 233.
[3] N. Narukage *et al*., Applied Optics **54** (2015) 2080.
[4] N. Narukage *et al*., UVSOR Activity Report 2012 **40** (2013) 46.
[5] N. Narukage *et al*., UVSOR Activity Report 2012 **40** (2013) 47.
[6] R. Ishikawa *et al*., Solar Physics **289** (2014) 4727.

BL7B

The Improvement and Evaluation of VIS-VUV Ellipsometry

Y. Kubo[1], K. Fukui[1], K. Yamamoto[2], T. Saito[3] and T. Horigome[4]

[1]*Department of Electrical and Electronics Engineering, University of Fukui, Fukui 910-8507, Japan*

[2]*FIR Center, University of Fukui, Fukui 910-8507, Japan*

[3]*Department of Environment and Energy, Tohoku Institute of Technology, Sendai 982-8577, Japan*

[4]*UVSOR Facility, Institute for Molecular Science, Okazaki 444-8585, Japan*

Recently, the need for quantitative measurements of ultraviolet (UV) - vacuum UV (VUV) radiation is increasing with the expanding applications of the radiation for sterilization, curing, *etc*.. However, most widely used Si photodiodes, have a serious problem of degradation under UV exposure. To develop stable new UV detectors, accurate optical constants of alternative materials, especially of wide bandgap ones, composing a detector are necessary. Although commercially available spectroscopic ellipsometers (SE) are known as a powerful tool to obtain optical constants with high accuracy, the highest photon energy limit is typically in the near UV. Therefore, we are improving a visible (VIS) – VUV SE which is designed by an AIST group [1] to optimizing for the use at BL7B. In this report, we show present status of a VIS-VUV SE at BL7B.

Figure 1 shows the side view of VIS-VUV SE. In this SE, an oblique incident photodiode and a sample chamber are rotated along the incident beam axis (β and α rotations) instead of the rotations of an analyzer and a polarizer, respectively. Then, both rapid and accurate 5-axis adjustable mechanical system to align mechanical α rotation axis with the light axis is required. To realize computer controlled adjustable mounting at the narrow working space of BL7B, we design and construct a mount using parallel link mechanism. Measurement accuracy drastically increases after installing this mount.

Figure 2 shows both the refractive index *n* and the extinction coefficient *k* of Au mirror as a function of photon energy. Color symbols represent measurement results under various experimental conditions. The solid lines show the standard table data of Au [2] for comparison. Although measurement errors mainly affect the accuracy of extinction coefficient *k* according to the measurement principles, *k* shows good agreement with reference data in the whole measurement photon energy range. However, the accuracy of *n* is not enough at present and further improvement is needed, though absolute values of *n* are in agreement with rough surface Au thin film [3]

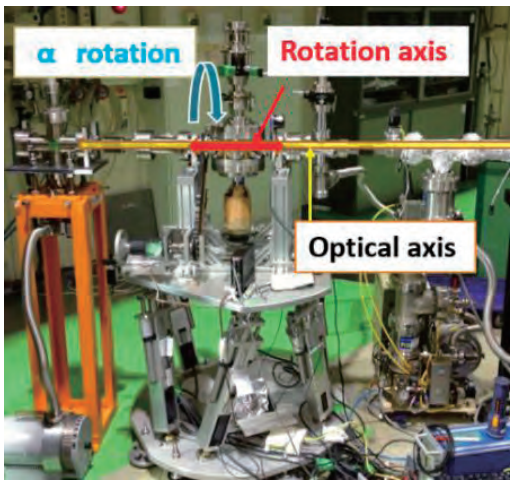

Fig. 1. Side view of a visible - vacuum ultraviolet spectroscopic ellipsometer at BL7B.

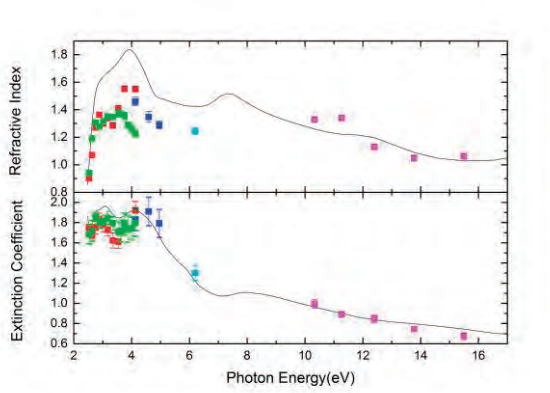

Fig. 2. Photon energy dependences of both refractive index and extinction coefficient of Au mirror.

[1] T. Saito, M. Yuri and H. Onuki, Rev. Sci. Instrum. **66** (1995) 1570.

[2] D.E. Gray *ed*., *American Institute of Physics Handbook 3rd edition* (McGraw-Hill, 1972) **6**-136.

[3] M. L. Theye, Phys. Rev. B **2** (1970) 3060.

UVSOR User 3